

# We are IntechOpen, the world's leading publisher of Open Access books Built by scientists, for scientists

## 4,800

Open access books available

## 122,000

International authors and editors

## 135M

Downloads

Our authors are among the

## 154

Countries delivered to

## TOP 1%

most cited scientists

## 12.2%

Contributors from top 500 universities

**WEB OF SCIENCE™**Selection of our books indexed in the Book Citation Index  
in Web of Science™ Core Collection (BKCI)

Interested in publishing with us?  
Contact [book.department@intechopen.com](mailto:book.department@intechopen.com)

Numbers displayed above are based on latest data collected.

For more information visit [www.intechopen.com](http://www.intechopen.com)

## Phase Diagram and Waterlike Anomalies in Core-Softened Shoulder-Dumbbell Complex Fluids

Paulo A. Netz<sup>1</sup>, Guilherme K. Gonzatti<sup>1</sup>, Marcia C. Barbosa<sup>2</sup>, Juliana Z. Paukowski<sup>2</sup>, Cristina Gavazzoni<sup>2</sup> and Alan Barros de Oliveira<sup>3</sup>

<sup>1</sup>*Instituto de Química, Universidade Federal do Rio Grande do Sul, Porto Alegre*

<sup>2</sup>*Instituto de Física, Universidade Federal do Rio Grande do Sul, Porto Alegre*

<sup>3</sup>*Departamento de Física, Universidade Federal de Ouro Preto, Ouro Preto  
Brazil*

### 1. Introduction

Water is not only by far the most important liquid in nature but also the one with the most puzzling behavior. Its density decreases upon cooling below 4 °C and the compressibility and specific heat increase anomalously by cooling. Water has also unusually high boiling, freezing and critical points and also a very high viscosity. In certain range of pressures, the diffusivity of water molecules increases with increasing pressure. Nevertheless, many very simple molecular water models proved to be able to reproduce several water anomalies (Angell et al., 2000; Errington & Debenedetti, 2001; Guillot, 2002; Kumar et al., 2005; Lynden-Bell, 2010; Netz, Starr, Barbosa & Stanley, 2004; Netz et al., 2001; Pi et al., 2009; Stanley et al., 2008). Consequently, very complex thermodynamic, dynamic or macroscopic features in principle could be captured in simple intermolecular model potentials.

In addition, some other complex materials also exhibit anomalous behavior. This is the case of  $\text{Se}_x\text{Te}_{1-x}$  (Thurn & Ruska, 1976), and  $\text{Ge}_{15}\text{Te}_{85}$  (Tsuchiya, 1991) which have density anomaly. Liquid sulfur displays a sharp minimum in the density (Sauer & Borst, 1967), related to a polymerization transition (Kennedy & Wheeler, 1983). Waterlike anomalies were also found in simulations for silica (Angell et al., 2000; Angell & Kanno, 1976; Poole et al., 1997; Sharma, Chakraborty & Chakravarty, 2006; Shell et al., 2002), silicon (Sastry & Angell, 2003) and  $\text{BeF}_2$  (Agarwal et al., 2007; Angell et al., 2000; Hemmer et al., 2001). Despite being successful in the description of many aspects of water and other anomalous materials behavior, however, none of these potentials could indeed reproduce all desired properties.

The understanding of the phase behavior of fluids based solely on the information about the intermolecular interactions remains as one of the biggest challenges in the statistical thermodynamics. The scientific community has already recognized that such big challenge demands a smart strategy: beginning with the simplest models.

It is recognized that the origin of the anomalies is related to the competition between open low-density and closed high-density structures, which depend on the thermodynamic state of the liquid (Krekelberg et al., 2008). In simple isotropic models, this competition is described by two preferred interparticle distances. This simple recipe gives rise to a myriad of models and

approaches (Almarza et al., 2009; Balladares & Barbosa, 2004; Buldyrev et al., 2002; Buldyrev & Stanley, 2003; de Oliveira & Barbosa, 2005; de Oliveira et al., 2007; de Oliveira, Franzese, Netz & Barbosa, 2008; de Oliveira, Netz & Barbosa, 2008; de Oliveira et al., 2009; 2006a;b; Fomin et al., 2008; Franzese et al., 2001; 2002; Gibson & Wilding, 2006; Hemmer & Stell, 1970; Henriques & Barbosa, 2005; Henriques et al., 2005; Jagla, 1998; Kurita & Tanaka, 2004; Netz, Raymundi, Camera & Barbosa, 2004; Pretti & Buzano, 2004; Scala et al., 2000; Skibinsky et al., 2004; Wilding & Magee, 2002; Xu et al., 2005).

Among these models, the core-softened shoulder potential (Cho et al., 1996; de Oliveira et al., 2006a;b; Netz, Raymundi, Camera & Barbosa, 2004) reproduces qualitatively water's structural, density and diffusion anomalies. This potential is built summing a Lennard-Jones potential and a displaced Gaussian term, as follows:

$$U^*(r) = 4 \left[ \left( \frac{\sigma}{r} \right)^{12} - \left( \frac{\sigma}{r} \right)^6 \right] + a \exp \left[ -\frac{1}{c^2} \left( \frac{r - r_0}{\sigma} \right)^2 \right], \quad (1)$$

Depending of the choice of  $a$ ,  $c$  and  $r_0$ , a whole family of potentials can be built, which shapes ranging from double well to a ramp-like shoulder (Netz, Raymundi, Camera & Barbosa, 2004). Molecular dynamics simulations using double well intermolecular potentials constructed with this function show anomalous behavior in the stable region of the phase diagram if the outer minimum is deeper than the inner minimum. In the case of a deeper inner minimum, anomalous behavior is also present but inside an unstable region. Another choice of parameters, yielding a ramp-like shoulder profile is  $a = 5.0$ ,  $r_0/\sigma = 0.7$  and  $c = 1.0$ , which result in stable fluid phases in a large portion of the phase diagram.

Using this potential, we found that the hierarchy of anomalies, i.e. the loci in the pressure-temperature phase diagram of the state points displaying anomalous behavior (de Oliveira et al., 2006a;b), is the same as in water (Errington & Debenedetti, 2001; Netz et al., 2001): the structurally anomalous region in the pressure-temperature phase diagram enclosing the region of dynamic (diffusivity) anomalies, that in its turn is enclosing region of the thermodynamic (density) anomalies. In principle this shoulder potential can represent in an effective and orientation-averaged way the interaction between water pentamers (Krekelberg et al., 2008) characterized by the presence of two structures – one open and one closed – as discussed above. Similarly, the thermodynamic and dynamic anomalies result from the competition between the two length scales associated with the open and closed structures. The open structure is favored by low pressures and the closed structure is favored by high pressures, but only becomes accessible at sufficiently high temperatures.

Even though core-softened potentials have been mainly used for modeling water (de Oliveira & Barbosa, 2005; de Oliveira et al., 2009; 2006a;b; Franzese, 2007; Gibson & Wilding, 2006; Xu et al., 2006; Yan et al., 2006; 2005), many other materials present the so called water-like anomalous behaviour. In this sense, it is reasonable to use core-softened potentials as the building blocks of a broader class of materials which we can classify as anomalous fluids. One interesting aspect in this investigation is the role of multiple length scales and of anisotropy. It has been shown that the presence of many length scales in a spherical symmetric potential leads to only one region in the pressure-temperature phase-diagram with thermodynamic and dynamic anomalies (Netz et al., 2006) because actually only the smaller and the larger scales compete.

Obviously anisotropic systems are not only more complicated but the addition of other degrees of freedom result in a richer phase-diagram. For instance diatomic particles interacting through a Lennard-Jones potential (Kriebel & Winkelmann, 1996; Sumi et al.,

2004) exhibit a solid phase that occupies higher pressures and temperatures in the pressure-temperature phase diagram. In the case of the solid phase, the diatomic particles exhibit two close-packed arrangements instead of one as observed in the monoatomic Lennard-Jones (Vega et al., 2003). Therefore, it is expected that the dimeric system interacting through two length scales potential might have a phase-diagram with a larger solid phase region in the pressure-temperature phase diagram than the one occupied by the solid phase in the monomeric system.

In the recently proposed model of dimeric molecules linked as rigid dumbbells, interacting with the shoulder potential described above (de Oliveira et al., 2010) the anisotropy due to the dumbbell leads indeed to a much larger solid phase and to the appearance of a liquid crystal phase. This system has a peculiar phase behavior: by isothermal increase of the pressure at moderate temperatures, the system, beginning in the fluid phase, becomes solid, at high pressures it becomes fluid again and by further increase of the pressure it becomes liquid-crystal-like before becoming a solid.

The regions of thermodynamic, dynamic and structural anomalies display the same hierarchy as in the monomeric case. In general, the range of pressures and temperatures occupied by these anomalous regions are larger than those observed in the monomeric case. The differences are more pronounced for the regions of diffusion and structural anomalies and not so large for the thermodynamic anomalies.

These results showed that the dimeric particles interacting with the core softened shoulder potential have a different behavior when compared with the monomeric particles with the same interaction potential. This raises the following question: how to quantify the influence of the anisotropy, i.e. what is the role of the strength of anisotropy, the interparticle separation  $\lambda$ , on the phase and anomalous behavior?

We consider a set of  $N/2$  dimeric molecules formed each by two spherical particles of diameter  $\sigma$ , linked rigidly in pairs with the distance of  $\lambda$  between their centers of mass, as depicted in Fig. 1. Each particle within a dimer interacts with all particles belonging to other dimers with the intermolecular continuous shoulder potential (de Oliveira et al., 2006b) given by equation 1 with the parameters:  $a = 5.0$ ,  $r_0/\sigma = 0.7$ ,  $c = 1.0$  and comparing several values of  $\lambda$ .

In the following section we describe some details of the simulation methodology, the choice of state points and the methods of analysis and quantification of the anomalous behavior. In the next section, detailed results from simulations using  $\lambda = 0.50$  are compared with the previously simulated system with  $\lambda = 0.20$ . The results pointed out to further simulations with other values of  $\lambda$ , which are also discussed in this section. Finally, in the conclusions section, a survey of all we have learnt from this system is given, as well as we point out some perspectives.

## 2. Methods

We performed molecular dynamics simulations in the canonical ensemble using  $N = 500$  particles (250 dimers) in a cubic box with periodic boundary conditions, interacting with the intermolecular potential described above. The cutoff radius was set to 5.5 length units. Pressure, temperature, density, and diffusion are calculated in dimensionless units, as detailed elsewhere (de Oliveira et al., 2010). We first compared the previous (de Oliveira et al., 2010) results, obtained with the choice of  $\lambda/\sigma = 0.20$  with a new choice  $\lambda/\sigma = 0.50$ , in a broad range of temperatures ( $0.10 \leq T^* \leq 3.00$ ) and densities ( $0.10 \leq \rho^* \leq 0.50$ ). In order to follow the trend of the anomalies on lambda, several additional sets of simulations in a rather small

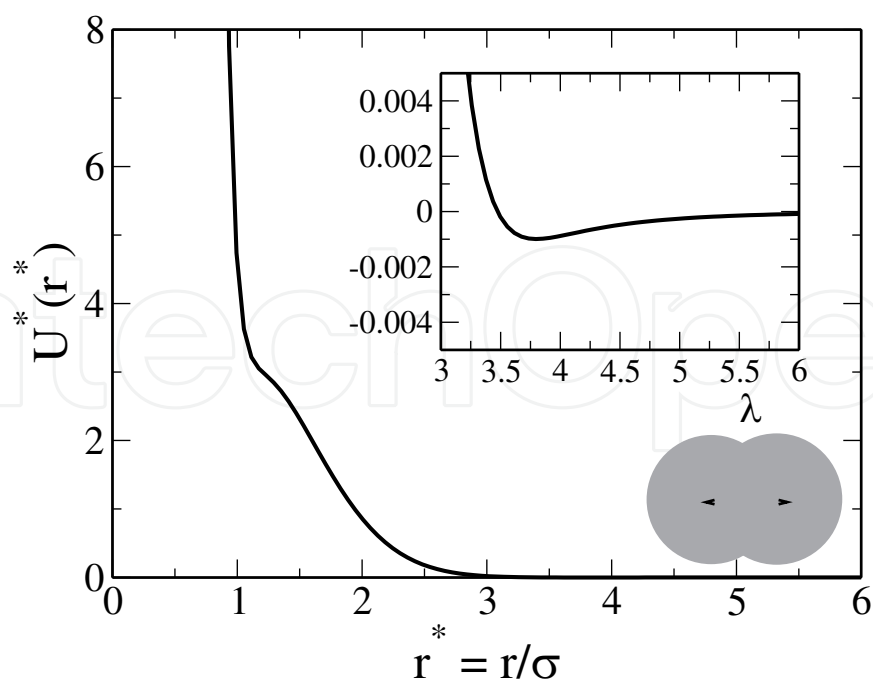


Fig. 1. Effective potential versus distance, in reduced units.

region of the phase diagram ( $0.60 \leq T^* \leq 0.94$  and  $0.20 \leq \rho^* \leq 0.28$ ) were carried out, for  $\lambda/\sigma = 0.10, 0.30, 0.40$  and  $0.70$ .

Thermodynamic and dynamic properties were calculated over 700 000 steps after previous 200 000 equilibration steps. The time step was 0.001 in reduced units, the time constant of the Berendsen thermostat (Berendsen et al., 1984) was 0.1 in reduced units. The internal bonds between the particles in each dimer remain fixed using the SHAKE (Ryckaert et al., 1977) algorithm, with a tolerance of  $10^{-12}$  and maximum of 100 interactions for each bond.

The stability of the systems was checked analyzing the dependence of pressure on density and also by visual analysis of the final structure, searching for cavitation. The structure of the system was characterized using the intermolecular radial distribution function,  $g(r)$  (RDF), which does not take into account the correlation between atoms belonging to the same molecule. The diffusion coefficient was calculated using the slope of the least square fit to the linear part of the mean square displacement,  $\langle r^2(t) \rangle$  (MSD), averaged over different time origins. Both the  $g(r)$  and  $\langle r^2(t) \rangle$  were computed taking the origin as the center of mass of a dimer. The phase boundary between solid and fluid phase was mapped by analysis of the change of the pattern of the mean squared displacement and radial distribution function. For the quantification of the structural anomaly we use the translational order parameter  $t$  (Errington & Debenedetti, 2001), given by

$$t \equiv \frac{1}{\xi_c} \int_0^{\xi_c} |g(\xi) - 1| d\xi, \quad (2)$$

which decreases upon increasing density in the structurally anomalous region. Here  $\xi \equiv r\rho^{1/3}$  is the distance  $r$  in units of the mean interparticle separation, computed by the center of mass of the dimers,  $\rho^{-1/3}$ ,  $\xi_c$  is the cutoff distance set to half of the simulation box times  $\rho^{-1/3}$ .  $g(\xi)$  is the radial distribution function as a function of the (reduced) distance  $\xi$  from a reference particle. For an ideal gas  $g = 1$  and  $t = 0$ . In the crystal phase  $g \neq 1$  over long distances and  $t$  is large.

In a previous work we showed that (de Oliveira et al., 2010), depending on the chosen temperature and density, the system could be in a fluid phase metastable with respect to the solid phase. In order to check this case, for  $\lambda/\sigma = 0.50$ , two sets of simulations were carried out, one with a ordered crystalline initial configuration and other with a liquid configuration obtained from previous equilibrium simulations. No noticeable differences were detected in the results of both sets.

### 3. Results

We carried out a detailed set of simulations of rigid dumbbells interacting with the potential 1 with  $\lambda/\sigma = 0.50$ . In order to locate the anomalous regions for this system, the following methodology was adopted.

First of all, it is needed to locate the phase boundary, i.e. the loci in the phase diagram separating the solid and fluid phases. This was determined by the change of pattern in the mean square displacement and radial distribution function. Fig. 2 shows that, for a chosen fixed density ( $\rho = 0.22$  in this figure), the system becomes fluid for temperatures above  $T = 0.39$ , as can be seen by the abrupt change of the slope of the mean square displacement and the change of a solid-like radial distribution function below this temperature to a fluid-like  $g(r)$  above that. This transition was independent of the starting configuration: simulations starting from the ordered crystalline initial configuration and from a previously equilibrated liquid configuration showed the same behavior. For other densities the location of the phase boundary was done in the same way.

Second, in order to map the region of thermodynamic anomalies, one has to locate the temperature of maximum density, TMD. The TMD was determined plotting the pressure against the temperature along isochores and locating the minima, as shown in Fig. 3. The isochores located between  $2.0 < P^* < 3.5$  have minimum at a certain temperature and pressure corresponding to a temperature of maximum density (TMD) at a given  $P^*$ .

Third, the region of diffusion anomalies is defined as the region where the mobility behaves anomalously, increasing  $D$  with increasing density. Indeed, for  $T^* > 0.65$ , the plot of the diffusion coefficient  $D$  against the density  $\rho$  along isotherms shows the same anomalous behavior (see Figure 3) already known for the waterlike core-softened shoulder monomeric (de Oliveira et al., 2006a;b) and dimeric (de Oliveira et al., 2010) systems. For low densities  $\rho < \rho_{D\min}$   $D$  decreases with increasing  $\rho$  (normal behavior); for intermediate densities  $\rho_{D\min} < \rho < \rho_{D\max}$ ,  $D$  increases with increasing  $\rho$  (anomalous behavior) and for high densities  $\rho > \rho_{D\max}$ , the behavior turns out to be the same of the normal fluids. For each temperature there is a  $\rho_{D\min}$  and a  $\rho_{D\max}$  and consequently a  $P_{D\min}(T)$  and a  $P_{D\max}(T)$ . The line of  $P_{D\max}(T)$  in the  $P$ - $T$  phase diagram illustrated in Fig. 5 is similar to the diffusivity maxima observed in experiments for water as well as in simulations of water (Errington & Debenedetti, 2001; Mittal et al., 2006; Netz et al., 2001), silica, (Poole et al., 1997; Sharma, Mudi & Chakravarty, 2006; Shell et al., 2002), other isotropic potentials (Xu et al., 2006; Yan et al., 2006; 2005) and for the potential Fig. 1 in the case in which the particles are monomeric (de Oliveira et al., 2006b). The line of  $P_{D\min}(T)$  is also shown in Fig. 5. The region of diffusion anomaly in the  $P^*$ - $T^*$  phase diagram is bounded by  $P_{D\min}(T)$  and  $P_{D\max}(T)$ .

Finally, the location of the structurally anomalous region demands mapping the extrema in the translational order parameter  $t$ . Fig. 4 shows the behavior of  $t$  along isotherms against density. It is expected, for normally behaved fluids, the increase of translational order parameter with increasing compression (as in the red and blue portions of the isotherms). The region where  $t$  decreases with increasing compression (delimited by the maximum and minimum) is shown

in black and corresponds to the structurally anomalous region. For low temperatures, the behavior is strikingly anomalous, stronger than in the monomeric case. It is also shown the typical pattern in the radial distribution functions, corresponding to the three regions seen in the figure. For low densities, the compression leads to an increase on the first peak of the radial distribution function, thus increasing  $t$ . For intermediate densities, a new, short range peak appears. The intensity of this inner peak increases and the former first peak (now termed the second peak) decreases in intensity. This competition is the main characteristic of the structurally anomalous region. Finally, a normal behavior is recovered at very high densities, because the inner peak dominates and grows leading to the increase in  $t$ .

Fig. 5 shows the pressure-temperature phase diagram of the shoulder-dumbbell system with the parameters described above and with the choice of  $\lambda/\sigma = 0.5$ . For comparison, it is also shown the corresponding phase diagram obtained previously (de Oliveira et al., 2010) with  $\lambda/\sigma = 0.2$ . For both cases, two solid regions are clearly seen, as well as fluid phases with different densities.

The boundaries of the anomalous regions depend clearly on  $\lambda$ . The solid-fluid phase boundary and the TMD are shifted towards lower temperatures and slightly higher pressures with the increase of  $\lambda$ . The high-temperature limit of the boundary of the region of diffusion anomalies becomes also shifted towards lower temperatures, whereas the lower-temperature part of this regions becomes broader. The structurally anomalous region shrinks with increasing  $\lambda$ .

In order to confirm the influence of  $\lambda$  on the phase diagram and regions of anomalous behavior, we carried out several simulations restricted to the small region in the phase diagram between the densities  $\rho = 0.20$  and  $\rho = 0.28$  (which correspond roughly to  $2 < P^* < 4$ ) and temperatures  $T = 0.60$  and  $T = 0.94$ . Figure 6 shows the solid-fluid phase boundary for the systems with  $\lambda/\sigma = 0.10, 0.20, 0.40, 0.50$  and  $0.70$ . The increase of the interparticle separation shifts the solid-fluid phase boundary to lower temperatures.

Figure 7 show the radial distribution functions for a chosen state point (density 0.20 and temperature 0.60) as a function of  $\lambda$ . The smaller values of  $\lambda$  tend to increase the solid-like nature of the system.

Comparing the results of the simulations corresponding to the several values of  $\lambda$  with the results of the monomeric shoulder-dumbbell simulations, we see an unexpected non-monotonic behavior. The effect of the introduction of a rather small anisotropy due to the dimeric nature of the particle (small values of the interparticle separation  $\lambda$ ) leads to the increase of the size of the regions of anomalies (de Oliveira et al., 2010). Nevertheless, the increase of  $\lambda$  shrinks those regions.

For very high densities, however, the boundary between solid and liquid phases is not sharp and a broad metastable region exhibiting liquid-crystal-like behavior is found. This state can be recognized by the comparison of the mean square displacement and radial distribution function for several temperatures with a fixed density. In this case there is no clear-cut change of pattern as the state point moves from solid to liquid (as in Figure 2 and it is seen, instead, a seemingly contradictory liquid-like mean square displacement and solid-like radial distribution function (see Fig 8).

This liquid-crystal-like behavior was also found in the shoulder-dumbbell system with  $\lambda/\sigma = 0.20$  (de Oliveira et al., 2010). In this state the particles have a crystal-like ordering, but diffuse as a one-dimensional string.

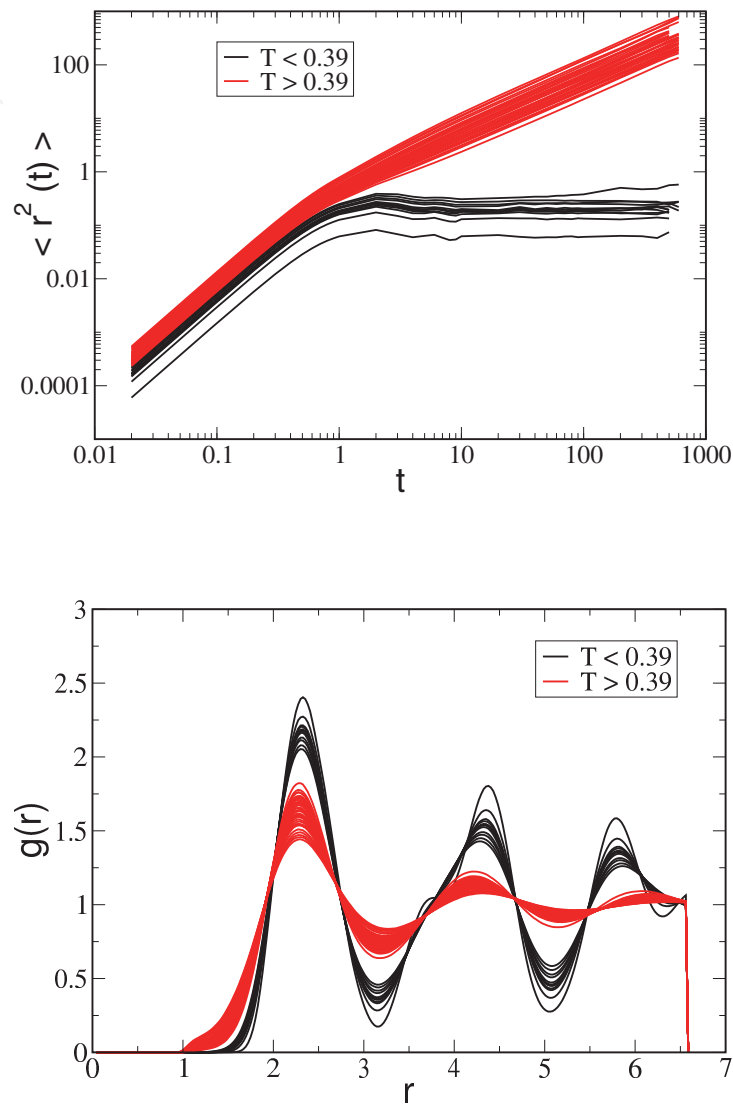


Fig. 2. Mapping the phase boundary between solid and fluid by the change of profile in the mean square displacement (a) and radial distribution function (b) for rigid dumbbells with interatomic separation  $\lambda/\sigma = 0.50$  and density 0.22.



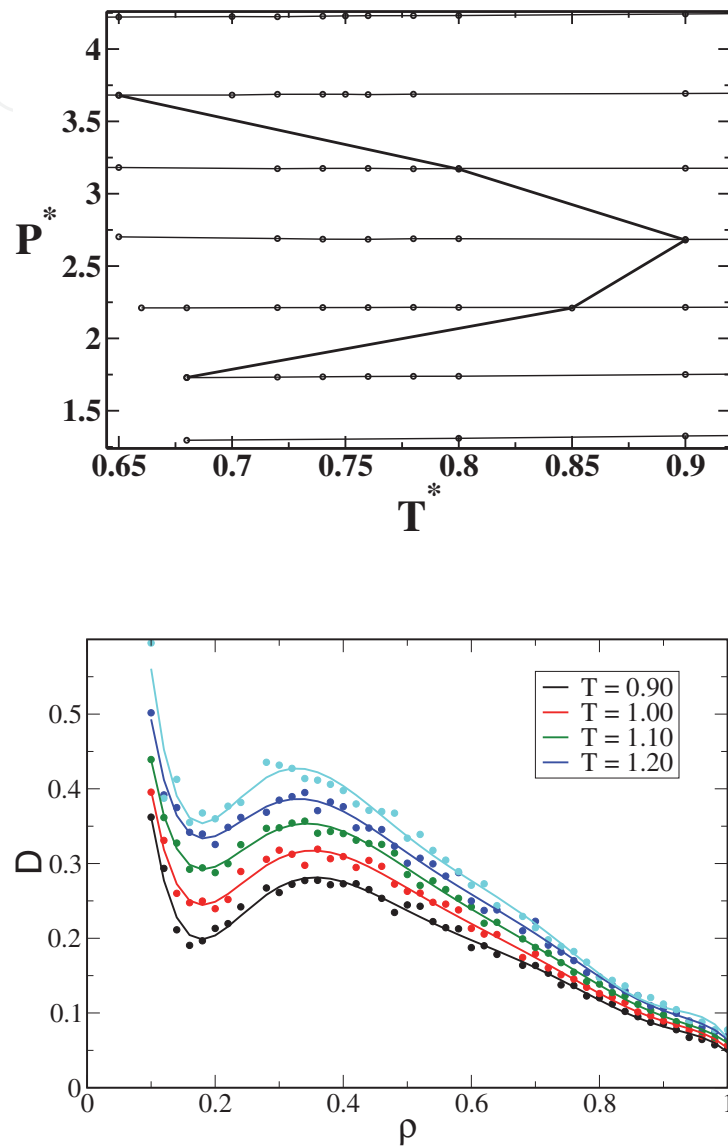


Fig. 3. Locating the TMD by the minimum of pressure along isochors (a) and the region of diffusion anomaly (b) for rigid dumbbells with interatomic separation  $\lambda/\sigma = 0.50$ .

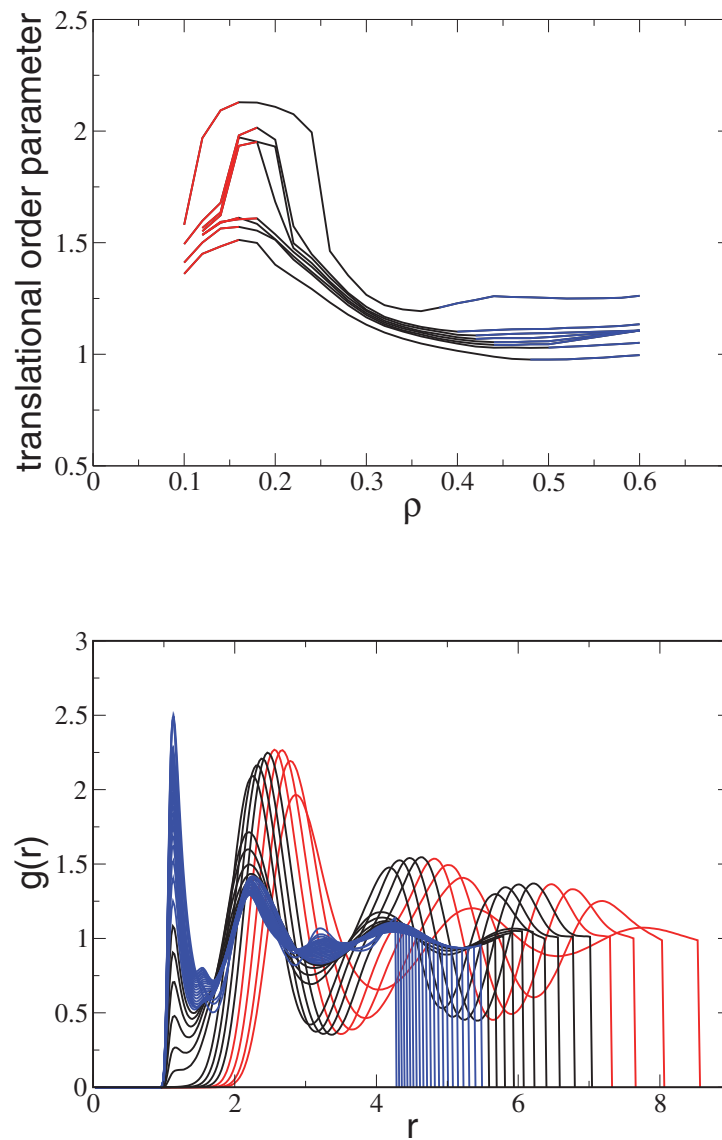


Fig. 4. (a) Translational order parameter for rigid dumbbells with interatomic separation  $\lambda/\sigma = 0.50$  as a function of density for temperatures  $T = 0.30, 0.40, 0.42, 0.44, 0.46, 0.48, 0.50$  and  $0.60$  (from top to bottom); (b) radial distribution functions ( $g(r)$ ) for a fixed temperature  $T = 0.30$  and several densities. The colors correspond to the densities where the translational order parameter increases (red), decreases (black) or increases (blue) under increasing density, as in (a).

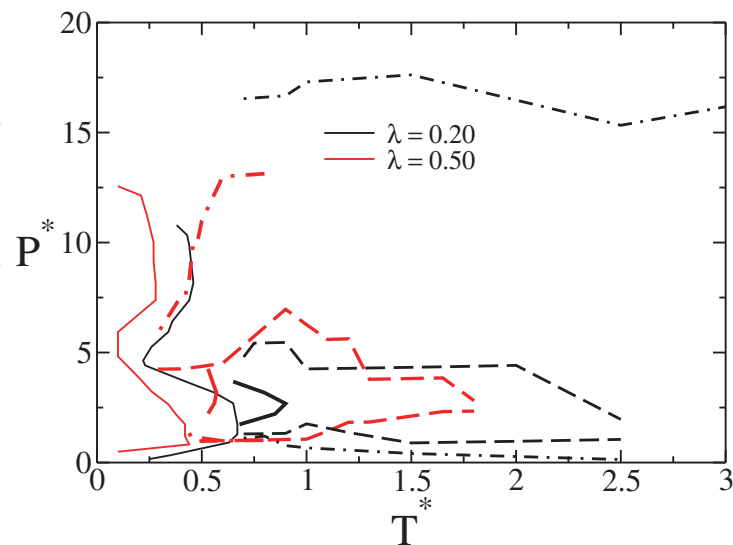


Fig. 5. Pressure versus temperature phase diagram of the potential illustrated in Figure 1 for rigid dumbbells with interatomic separation  $\lambda/\sigma = 0.20$  and  $\lambda/\sigma = 0.50$ . The thin solid lines represent the boundaries between the fluid and the solid phases, the bold solid line, the TMD's lines, the dashed lines represent the D extrema lines and the dotted-dashed lines the boundary of the structurally anomalous region.

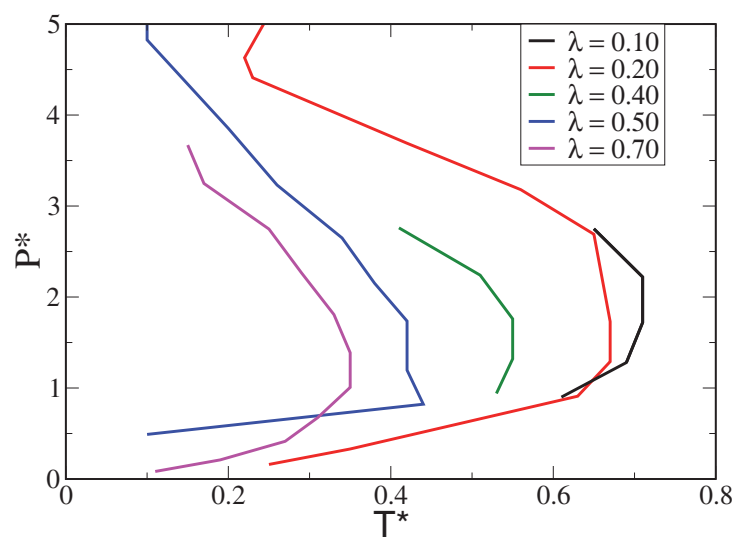


Fig. 6. Phase boundary for systems with  $\lambda/\sigma = 0.10, 0.20, 0.40, 0.50$  and  $0.70$ .

IntechOpen

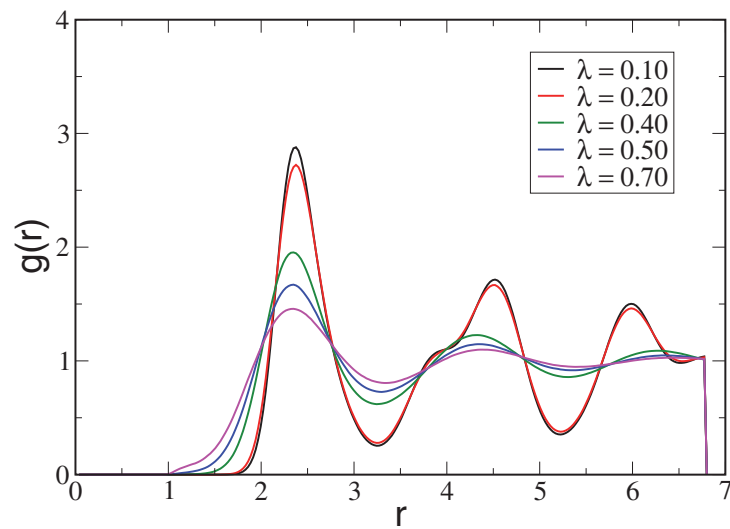


Fig. 7. Radial distribution functions for a chosen state point (density 0.20 and temperature 0.60) showing the influence of the interparticle separation  $\lambda$  on the structure.

IntechOpen

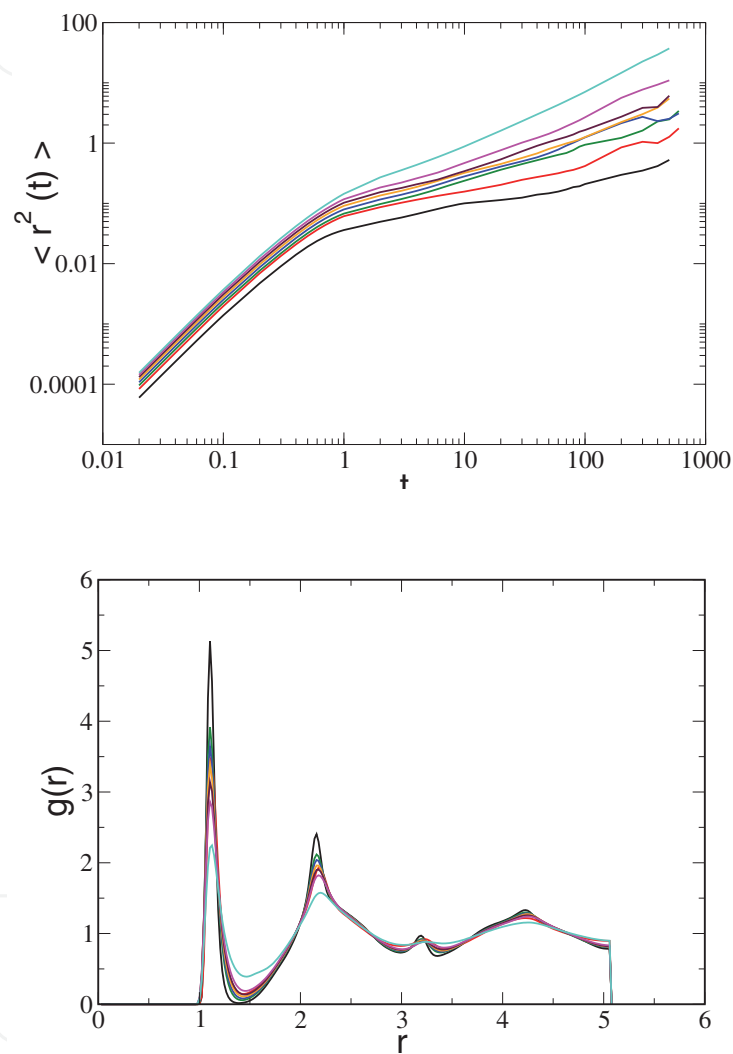


Fig. 8. Mean square displacement (a) and radial distribution function (b) for rigid dumbbells with interatomic separation  $\lambda/\sigma = 0.50$  and density 0.48. The curves show  $\langle r^2 \rangle$  or  $g(r)$  for temperatures  $T = 0.10$  (black), 0.12, 0.14, 0.16, 0.18, 0.20, 0.22, 0.24 and 0.26 (turquoise).

#### 4. Conclusions

In this work we have simulated a system consisting of rigid dimers in which each monomer interacts with monomers from the other dimers through a core-softened shoulder potential. In order to check how the anisotropy induced by the dimeric structure affects the presence of density, diffusion and structural anomalies, we have obtained the pressure temperature phase diagram, the diffusion constant and the structural order parameter of the system for different  $\lambda$ , distance between the bonded particles in each dimer, values.

The understanding of this effect is a fundamental step towards modeling more complex systems such as polymers in which anomalies would be present.

We found that this system has thermodynamic, dynamic and structural anomalies similar to the anomalies present in the monomeric case, but the size of the anomalous region in the pressure temperature phase diagram is dependent on the value of  $\lambda$ .

In particular we found that in the range  $0.1 < \lambda < 0.7$  the pressures and the temperatures of the melting line decrease with increasing  $\lambda$ . This result is consistent with the idea that the anisotropy enhanced by large values of  $\lambda$  made it difficult for the system to reach the proper solid configuration. Any small thermal motion disrupts the structure that finds it easier to be in a solid phase. The same argument also explains why the region in the pressure temperature phase diagram occupied by the density, diffusion and structural anomalous regions is smaller for large  $\lambda$  values than for smaller values. As the anisotropy becomes larger, the competition between the two length scales that is responsible for the anomalies becomes less important for the organization of the particles than the dimer scale. As a result the anomalous regions do exist only for a narrow range of pressures and temperatures where the dimeric scale does not prevail.

#### 5. References

- Agarwal, M., Sharma, R. & Chakravarty, C. (2007). Ionic melts with waterlike anomalies: Thermodynamic properties of liquid BeF<sub>2</sub>, *J. Chem. Phys.* 127: 164502.
- Almarza, N. G., Capitan, J. A., Cuesta, J. A. & Lomba, E. (2009). Phase diagram of a two-dimensional lattice gas model of a ramp system, *J. Chem. Phys.* 131: 124506.
- Angell, C. A., Bressel, R. D., Hemmatti, M., Sare, E. J. & Tucker, J. C. (2000). Water and its anomalies in perspective: tetrahedral liquids with and without liquid-liquid phase transitions., *Phys. Chem. Chem. Phys.* 2: 1559.
- Angell, C. A. & Kanno, H. (1976). Density maxima in high-pressure supercooled water and liquid silicon dioxide, *Science* 193: 1121.
- Balladares, A. & Barbosa, M. C. (2004). Density anomaly in core-softened lattice gas, *J. Phys.: Cond. Matter* 16: 8811.
- Berendsen, H. J. C., Postuma, J. P. M., van Gunsteren, W. F., DiNola, A. & Haak, J. R. (1984). Molecular dynamics with coupling to an external bath, *J. Chem. Phys.* 81: 3684–3690.
- Buldyrev, S. V., Franzese, G., Giovambattista, N., Malescio, G., Sadr-Lahijany, M. R., Scala, A., Skibinsky, A. & Stanley, H. E. (2002). Models for a liquid-liquid phase transition, *Physica A* 304: 23.
- Buldyrev, S. V. & Stanley, H. E. (2003). A system with multiple liquid-liquid critical points, *Physica A* 330: 124.
- Cho, C. H., Singh, S. & Robinson, G. W. (1996). Liquid water and biological systems: the most important problem in science that hardly anyone wants to see solved, *Faraday Discuss.* 103: 19.

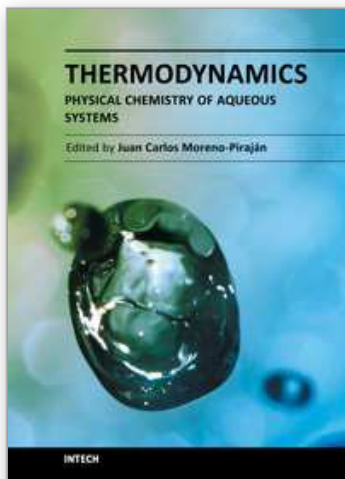
- de Oliveira, A. B. & Barbosa, M. C. (2005). Density anomaly in a competing interactions lattice gas model, *J. Phys.: Cond. Matter* 17: 399.
- de Oliveira, A. B., Barbosa, M. C. & Netz, P. A. (2007). Interplay between structure and density anomaly for an isotropic core-softened ramp-like potential, *Physica A* 386: 744.
- de Oliveira, A. B., Franzese, G., Netz, P. A. & Barbosa, M. C. (2008). Waterlike hierarchy of anomalies in a continuous spherical shouldered potential, *J. Chem. Phys* 128: 064901.
- de Oliveira, A. B., Netz, P. A. & Barbosa, M. C. (2008). Which mechanism underlies the water-like anomalies in core-softened potentials?, *Euro. Phys. J. B* 64: 481.
- de Oliveira, A. B., Netz, P. A. & Barbosa, M. C. (2009). An ubiquitous mechanism for water-like anomalies, *Europhys. Lett.* 85: 36001.
- de Oliveira, A. B., Netz, P. A., Colla, T. & Barbosa, M. C. (2006a). Structural anomalies for a three dimensional isotropic core-softened potential, *J. Chem. Phys.* 125: 124503.
- de Oliveira, A. B., Netz, P. A., Colla, T. & Barbosa, M. C. (2006b). Thermodynamic and dynamic anomalies for a three-dimensional isotropic core-softened potential, *J. Chem. Phys.* 124: 084505.
- de Oliveira, A. B., Neves, E. B., C., G., Paukowski, J. Z., Netz, P. A. & Barbosa, M. C. (2010). Liquid crystal phase and waterlike anomalies in a core-softened shoulder-dumbbells system, *J. Chem. Phys* 132: 164505.
- Errington, J. R. & Debenedetti, P. D. (2001). Relationship between structural order and the anomalies of liquid water, *Nature (London)* 409: 318.
- Fomin, D. Y., Frenkel, D., Gribova, N. V. & Ryzhov, V. N. (2008). Quasibinary amorphous phase in a three-dimensional system of particles with repulsive-shoulder interactions, *J. Chem. Phys.* 127(064512).
- Franzese, G. (2007). Differences between discontinuous and continuous soft-core attractive potentials: The appearance of density anomaly, *J. Mol. Liq.* 136(3): 267.
- Franzese, G., Malescio, G., Skibinsky, A., Buldyrev, S. V. & Stanley, H. E. (2001). Generic mechanism for generating a liquid-liquid phase transition, *Nature (London)* 409: 692.
- Franzese, G., Malescio, G., Skibinsky, A., Buldyrev, S. V. & Stanley, H. E. (2002). Metastable liquid-liquid phase transition in a single-component system with only one crystal phase and no density anomaly, *Phys. Rev. E* 66: 051206.
- Gibson, H. M. & Wilding, N. B. (2006). Metastable liquid-liquid coexistence and density anomalies in a core-softened fluid, *Phys. Rev. E* 73: 061507.
- Guillot, B. (2002). A reappraisal of what we have learnt during three decades of computer simulations on water, *J. Mol. Liq.* 101: 219.
- Hemmer, P. C. & Stell, G. (1970). Fluids with several phase transitions, *Phys. Rev. Lett.* 24: 1284.
- Hemmer, P. C., Velasco, E., Medeiros, L., Navascués, G. & Stell, G. (2001). Solid-solid transitions induced by repulsive interactions, *J. Chem. Phys.* 114: 2268.
- Henriques, V. B. & Barbosa, M. C. (2005). Liquid polymorphism and density anomaly in a lattice gas model, *Phys. Rev. E* 71: 031504.
- Henriques, V. B., Guisconi, N., Barbosa, M. A., Thielo, M. & Barbosa, M. C. (2005). Liquid polyamorphism and double criticality in a lattice gas model, *Mol. Phys.* 103: 3001.
- Jagla, E. A. (1998). Phase behavior of a system of particles with core collapse, *Phys. Rev. E* 58: 1478.
- Kennedy, S. J. & Wheeler, J. C. (1983). On the density anomaly in sulfur at the polymerization transition, *J. Chem. Phys.* 78: 1523.
- Krekelberg, W. P., Mittal, J., Ganesan, V. & Truskett, T. M. (2008). Structural anomalies of fluids: Origins in second and higher coordination shells, *Phys. Rev. E* 77: 041201.

- Kriebel, C. & Winkelmann, J. (1996). Polarizable dipolar two-center Lennard-Jones fluids: Computer simulations and equation of state, *J. Chem. Phys.* 105: 9316.
- Kumar, P., Buldyrev, S. V., Sciortino, F., Zaccarelli, E. & Stanley, H. E. (2005). Static and dynamic anomalies in a repulsive spherical ramp liquid: Theory and simulation, *Phys. Rev. E* 72: 021501.
- Kurita, R. & Tanaka, H. (2004). Critical-like phenomena associated with liquid-liquid transition in a molecular liquid, *Science* 306: 845.
- Lynden-Bell, R. M. (2010). Towards understanding water: simulation of modified water models, *Journal of Physics, Condensed Matter* 22: 284107.
- Mittal, J., Errington, J. R. & Truskett, T. M. (2006). Quantitative link between single-particle dynamics and static structure of supercooled liquids, *J. Phys. Chem. B* 110: 18147.
- Netz, P. A., Buldyrev, S., Barbosa, M. C. & Stanley, H. E. (2006). Thermodynamic and dynamic anomalies for dumbbell molecules interacting with a repulsive ramplike potential, *Physical Review E* 73: 061504.
- Netz, P. A., Raymundi, J. F., Camera, A. S. & Barbosa, M. C. (2004). Dynamic anomalies of fluids with isotropic doubled-ranged potential, *Physica A* 342: 48.
- Netz, P. A., Starr, F., Barbosa, M. C. & Stanley, H. E. (2004). Computer simulation of dynamical anomalies in stretched water, *Brazilian Journal of Physics* 34: 24.
- Netz, P. A., Starr, F. W., Stanley, H. E. & Barbosa, M. C. (2001). Static and dynamic properties of stretched water, *J. Chem. Phys.* 115: 344.
- Pi, H. L., Aragonés, J. L., Vega, C., Noya, E. G., Abascal, J. L. F., Gonzalez, M. A. & McBride, C. (2009). Anomalies in water as obtained from computer simulations of the tip4p/2005 model: density maxima, and density, isothermal compressibility and heat capacity minima, *Molecular Physics* 107: 365.
- Poole, P. H., Hemmati, M. & Angell, C. A. (1997). Comparison of thermodynamic properties of simulated liquid silica and water, *Phys. Rev. Lett.* 79: 2281.
- Pretti, M. & Buzano, C. (2004). Thermodynamic anomalies in a lattice model of water, *J. Chem. Phys.* 121: 11856.
- Ryckaert, J. P., Ciccotti, G. & Berendsen, H. J. C. (1977). Numerical integration of the cartesian equations of motion of a system with constraints: molecular dynamics of n-alkanes, *J. Comput. Phys.* 23: 327.
- Sastry, S. & Angell, C. A. (2003). Liquid-liquid phase transition in supercooled silicon, *Nature Mater.* 2: 739.
- Sauer, G. E. & Borst, L. B. (1967). Lambda transition in liquid sulfur, *Science* 158: 1567.
- Scala, A., Sadr-Lahijany, M. R., Giovambattista, N., Buldyrev, S. V. & Stanley, H. E. (2000). Applications of the Stell-Hemmer potential to understanding second critical points in real systems, *J. Stat. Phys.* 100: 97.
- Sharma, R., Chakraborty, S. N. & Chakravarty, C. (2006). Entropy, diffusivity, and structural order in liquids with waterlike anomalies, *J. Chem. Phys.* 125: 204501.
- Sharma, R., Mudi, A. & Chakravarty, C. (2006). Diffusional anomaly and network dynamics in liquid silica, *J. Chem. Phys.* 125: 044705.
- Shell, M. S., Debenedetti, P. G. & Panagiotopoulos, A. Z. (2002). Molecular structural order and anomalies in liquid silica, *Phys. Rev. E* 66: 011202.
- Skibinsky, A., Buldyrev, S. V., Franzese, G., Malescio, G. & Stanley, H. E. (2004). Liquid-liquid phase transitions for soft-core attractive potentials, *Phys. Rev. E* 69: 061206.



- Stanley, H. E., Kumar, P., Franzese, G., Xu, L., Yan, Z., Mazza, M. G., Buldyrev, S. V., Chen, S. H. & Mallamace, F. (2008). Liquid polyamorphism: Possible relation to the anomalous behaviour of water, *European Physical Journal* 161: 1.
- Sumi, T., Shirahama, H. & Sekino, H. (2004). A density-functional study for the liquid-vapor coexistence curve of nitrogen fluid, *J. Chem. Phys.* 121: 1014.
- Thurn, H. & Ruska, J. (1976). Change of bonding system in liquid  $\text{Se}_{10}\text{Te}_{1.1}$  alloys as shown by density measurements, *J. Non-Cryst. Solids* 22: 331.
- Tsuchiya, T. (1991). The anomalous negative thermal expansion and the compressibility maximum of molten Ge-Te alloys, *J. Phys. Soc. Jpn.* 60: 227.
- Vega, C., McBride, C., de Mibuel, E., J., B. F. & Galindo, A. (2003). The phase diagram of the two center lennard-jones model as obtained from computer simulation and wertheim's thermodynamic perturbation theory, *J. Chem. Phys.* 118: 10696.
- Wilding, N. B. & Magee, J. E. (2002). Phase behavior and thermodynamic anomalies of core-softened fluids, *Phys. Rev. E* 66: 031509.
- Xu, L., Buldyrev, S., Angell, C. A. & Stanley, H. E. (2006). Thermodynamics and dynamics of the two-scale spherically symmetric jagla ramp model of anomalous liquids, *Phys. Rev. E* 74: 031108.
- Xu, L., Kumar, P., Buldyrev, S. V., Chen, S.-H., Poole, P., Sciortino, F. & Stanley, H. E. (2005). Relation between the widom line and the dynamic crossover in systems with a liquid-liquid phase transition, *Proc. Natl. Acad. Sci. U.S.A.* 102: 16558.
- Yan, Z., Buldyrev, S. V., Giovambattista, N., Debenedetti, P. G. & Stanley, H. E. (2006). Family of tunable spherically symmetric potentials that span the range from hard spheres to waterlike behavior, *Phys. Rev. E* 73: 051204.
- Yan, Z., Buldyrev, S. V., Giovambattista, N. & Stanley, H. E. (2005). Structural order for one-scale and two-scale potentials, *Phys. Rev. Lett.* 95: 130604.

IntechOpen



## **Thermodynamics - Physical Chemistry of Aqueous Systems**

Edited by Dr. Juan Carlos Moreno Piraján

ISBN 978-953-307-979-0

Hard cover, 434 pages

**Publisher** InTech

**Published online** 15, September, 2011

**Published in print edition** September, 2011

Thermodynamics is one of the most exciting branches of physical chemistry which has greatly contributed to the modern science. Being concentrated on a wide range of applications of thermodynamics, this book gathers a series of contributions by the finest scientists in the world, gathered in an orderly manner. It can be used in post-graduate courses for students and as a reference book, as it is written in a language pleasing to the reader. It can also serve as a reference material for researchers to whom the thermodynamics is one of the area of interest.

### **How to reference**

In order to correctly reference this scholarly work, feel free to copy and paste the following:

Paulo A. Netz, Guilherme K. Gonzatti, Marcia C. Barbosa, Juliana Z. Paukowski, Cristina Gavazzoni and Alan Barros de Oliveira (2011). Phase Diagram and Waterlike Anomalies in Core-Softened Shoulder-Dumbbell Complex Fluids, *Thermodynamics - Physical Chemistry of Aqueous Systems*, Dr. Juan Carlos Moreno Piraján (Ed.), ISBN: 978-953-307-979-0, InTech, Available from: <http://www.intechopen.com/books/thermodynamics-physical-chemistry-of-aqueous-systems/phase-diagram-and-waterlike-anomalies-in-core-softened-shoulder-dumbbell-complex-fluids>

**INTECH**  
open science | open minds

### **InTech Europe**

University Campus STeP Ri  
Slavka Krautzeka 83/A  
51000 Rijeka, Croatia  
Phone: +385 (51) 770 447  
Fax: +385 (51) 686 166  
[www.intechopen.com](http://www.intechopen.com)

### **InTech China**

Unit 405, Office Block, Hotel Equatorial Shanghai  
No.65, Yan An Road (West), Shanghai, 200040, China  
中国上海市延安西路65号上海国际贵都大饭店办公楼405单元  
Phone: +86-21-62489820  
Fax: +86-21-62489821

© 2011 The Author(s). Licensee IntechOpen. This chapter is distributed under the terms of the [Creative Commons Attribution-NonCommercial-ShareAlike-3.0 License](https://creativecommons.org/licenses/by-nc-sa/3.0/), which permits use, distribution and reproduction for non-commercial purposes, provided the original is properly cited and derivative works building on this content are distributed under the same license.

IntechOpen

IntechOpen